ACS Sustainable Chemistry & Engineering

Research Article

pubs.acs.org/journal/ascecg

Facile Preparation of MnO_2/Graphene Nanocomposites with Spent Battery Powder for Electrochemical Energy Storage

Jinxing Deng,[†] Xue Wang,[†] Xiaojuan Duan,[†] and Peng Liu*[,†,‡]

[†]State Key Laboratory of Applied Organic Chemistry and Key Laboratory of Nonferrous Metal Chemistry and Resources Utilization of Gansu Province, College of Chemistry and Chemical Engineering, Lanzhou University, Lanzhou 730000, China

[‡]Joint Research Center of Urban Resource Recycling Technology of Graduate School at Shenzhen, Tsinghua University and Shenzhen Green Eco-Manufacturer High-Tech, Shenzhen, 518055, China

ABSTRACT: A conception of "waste from the power should be used for the power" was established for sustainable energy development in the present work. Series of MnO_2/graphene nanocomposites have been prepared via a facile physical mixing method as the electrode materials for supercapacitors with the spent battery powder (SBP) as raw material, which was obtained from the spent Zn-MnO_2 acidic dry batteries via simple processing. The structure and morphology of the resulting composites were characterized by FT-IR, Raman, XRD, TEM, and SEM. The electrochemical tests showed that the as-obtained SBP had low impedance and excellent cyclic stability of retaining 100% of its initial capacitance after 1000 cycles. After the incorporation of the carbon substrates (graphene oxide (GO) or reduced graphene oxide (rGO)), the capacitance was enhanced more than 2 times the original SBP (66 F/g), which can be attributed to the synergistic effect of the carbon materials and the metal oxide. The present work would lead to new insight into the recycling of waste batteries.

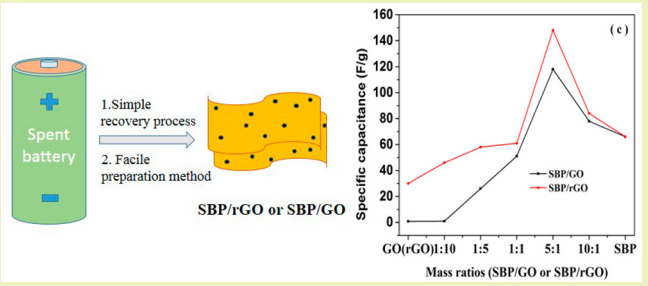

KEYWORDS: *Energy storage, Supercapacitor, Power waste, Graphene, Spent battery powder*

INTRODUCTION

Supercapacitors, an intermediate electrical energy storage system between batteries and dielectric capacitors, have attracted great attention due to their advantageous performances, such as reversibility, cycling stability, and high power densities, which are favored for high power electronics, medical electronics, transportation, et cetera.[1,2] According to the energy-storage mechanism, there are two types of supercapacitors. The electrical double layer capacitors (EDLC) possess a fast response and long cycle life but low specific capacitance, while the pseudocapacitors have high specific capacitance taking advantage of a fast and reversible electrochemical reaction of the redox active materials.[3] Recently, research for supercapacitive electrode materials has mainly focused on conducting polymers, carbons, and metal oxides.[1,4] Graphene and its derivatives have been conceived as extremely excellent electrode materials for supercapacitors because of their promising physical and chemical performance.[5,6] Also, as a pseudocapacitive electrode material, MnO_2 exhibits distinguished properties owing to its high electrochemical activity, low cost, abundance, and environmental friendliness.[7] However, MnO_2 cannot usually achieve its theoretical specific capacitance due to its electrochemical dissolution during cycling and poor electrical conductivity.[8] Fortunately, the metal oxide/graphene composite electrode materials could exhibit better electrochemical performance through a synergetic effect of graphene and metal oxides.

Up to date, there are mainly four methods developed for the synthesis of the metal oxide/graphene composite:

(i) The most widely used method is based on the adsorption or anchoring manganese species (Mn^{2+}) on the substrate (graphene oxide (GO)) acting as a nucleation center first through its oxygenated functional groups; subsequently the manganese oxide was formed *in situ* by a hydrothermal oxidation reaction in alkaline aqueous solution.[9] Gund et al. reported the preparation of a layer-by-layer structural GO/Mn_3O_4 composite through successive ionic layer van der Waals force and electrostatic of interaction between the opposite charges, and then the Mn^{2+} ions were oxidized into Mn_3O_4 in a NaOH solution.[10] Wang's group demonstrated the fabrication of the GO−MnO_2 nanocomposites by the intercalation and adsorption of Mn^{2+} onto the GO nanosheets, and then the growth of the MnO_2 nanocrystals onto the GO nanosheets was assisted by the oxidation with $KMnO_4$.[11]

(ii) The manganese oxide was fabricated in advance and then subjected to modification to enhance the interactions between the graphene sheets and metal oxide. Cheng et al. first prepared tetrabutylammonium (TBA^+)-exfoliated MnO_2 sheets, followed by a solution-phase assembly process of graphene sheets and MnO_2 to obtain the graphene/MnO_2 nanowire electrode

Received: January 25, 2015
Revised: May 16, 2015
Published: May 20, 2015

DOI: 10.1021/acssuschemeng.5b00305
ACS Sustainable Chem. Eng. 2015, 3, 1330−1338

materials with a high power density.[12] He and Zhu fabricated the graphene-wrapped MnO_2 nanocomposites via electrostatic interaction between graphene and the aminopropyltrimethoxysilane modified MnO_2 nanospheres.[13]

(iii) The MnO_2/graphene composites also can be prepared by a chemical or electrochemical deposition method. Yan et al. deposited MnO_2 onto the surface of graphene by a redox reaction, in which $KMnO_4$ was reduced to MnO_2 by the sacrifice of graphene carbon.[14] Similarly, Mn_3O_4 nanorods were well-dispersed onto the graphene substrate through the redox reaction process between $KMnO_4$ and ethylene glycol.[15] A graphene/manganese oxide composite with hierarchical structure has also been produced via potentiodynamic deposition.[16]

(iv) The simplest way is a physical mixing of colloidal metal oxide nanoparticles and rGO to prepare MnO_2−rGO nanocomposites with excellent cyclic stability and high specific capacitance.[17] Hsieh et al. also prepared SnO_2/rGO electrode materials just by mixing the SnO_2 powders and GO suspensions, followed by thermal reduction at 450 °C.[18] Nevertheless, among all these commonly used methods, the preparation processes are complex and consume lots of chemicals or energy. Therefore, it is meaningful to attempt to develop a cost-effective and easy operation for preparing the MnO_2/graphene supercapacitive electrode material.

It was reported that tons of toxic and hazardous metals had been produced by the discarding of millions of used batteries each year.[19] So, it is desirable and necessary to develop a simple and cost-effective process to recycle the waste batteries resources, which not only has positive effects on the environment but also might lead to advanced functional materials. Qu et al. prepared $Zn_xMn_{1-x}O$ nanoparticles from waste Zn−Mn batteries and investigated applications for photocatalytic degradation of bisphenol A. The photocatalyst exhibited an improved solar degradation efficiency.[20] Several technologies, such as pyrometallurgy, hydrometallurgy, and electrometallurgy, are still widely used to recover metals from the waste batteries; however, most of the processes need elevated temperatures and electricity to distill, precipitate, or deposit the metal components.[21,22]

Herein, we prepared the MnO_2/graphene nanocomposites as supercapacitive electrode materials via physical mixing spent battery powder (SBP) with different mass ratios of graphene oxide (GO) or the reduced one (rGO; Scheme 1). The well-dispersed fine SBP mainly containing graphite and MnO_2 nanoparticles was achieved from the spent Zn-MnO_2 acidic dry batteries by a simple method. The electrochemical tests showed that the SBP exhibited excellent cycling stability of keeping 100% of its original capacitance after 1000 CV cycles, and the specific capacitance increased to 150 F/g from 66 F/g after adding rGO with a mass ratio of SBP to rGO of 5:1. At the same time, it was found that the specific capacitances of the SBP/rGO nanocomposite electrodes were always higher than the SBP/GO nanocomposite electrodes with the same composition.

EXPERIMENTAL SECTION

Materials and Reagents. The origin graphite flake (Huatai Lubricant Sealling S&T Co. Ltd., Qingdao, China) and the spent Zn-MnO_2 acidic dry batteries (Shuanglu brand, China) were used as the main raw materials. The other reagents were analytical reagents and used without further purification. Doubly deionized water was used through all the processes.

Scheme 1. Schematic Illustration for Preparing the Nanocomposites via a Simple Recovery Process of the Spent Battery First and Then a Facile Physical Mixing at Room Temperature

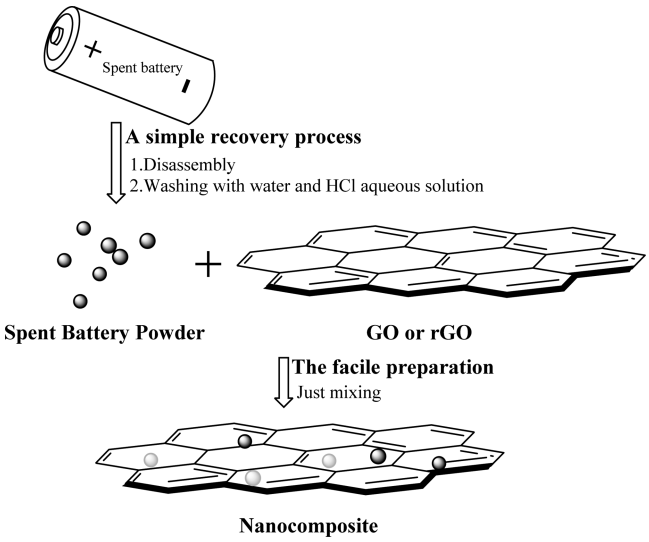

Recovery of SBP. Particular spent Zn-MnO_2 acidic dry batteries (1.5 V, electrolyte-NH_4Cl) were collected from the local sources. The desired positive electrode material (black spent battery powder) was first carefully separated from the plastic film, scrap paper, and outer metallic shell, and then the fine particles were obtained by manual milling. The black spent battery powder (denoted as SBP) thus collected was adequately washed with distilled water and HCl aqueous solution to remove certain species such as NH_4Cl, $ZnCl_2$, and MnOOH; finally the black SBP powder was dried at 70 °C.

Preparation of rGO Suspension. GO was prepared by a modified Hummers' method from expandable graphite.[23,24] A total of 1 g of expandable graphite flakes was added into 98% H_2SO_4 (23 mL) and stirred for 8 h after ultrasonication for 30 min. $KMnO_4$ (3 g) was gradually added to the above mixture; afterward, the mixture was stirred at 40 °C for 30 min and then at 70 °C for 1 h. Subsequently, 50 mL of deionized water was added to the mixture, which was subjected to 100 °C temperature conditions for 30 min. Next, deionized water (150 mL) and H_2O_2 (30% wt %, 10 mL) were added to terminate the reaction. The product was easily precipitated after a few minutes' standing due to the presence of acid (weakening the electrostatic repulsion between the GO sheets) and then washed first with 5% HCl aqueous solution. Finally, the product was washed with deionized water by repeating centrifugation and filtration until it was neutral, and a steady GO suspension was obtained after ultrasonication for 2 h.

The reduction of GO to graphene was performed in accordance with the process.[25] A total of 200 mL of the resulting GO homogeneous dispersion (0.25 mg/mL) was subjected to sonication for 30 min. Later, 44 μL of hydrazine aqueous solution (80 wt %) and 308 μL of ammonia aqueous solution (28 wt %) were added to the GO dispersion and then stirred at 97 °C for 1 h. The reduced graphene oxide (rGO) dispersion was produced by reduced pressure distillation to remove water and washed several times with deionized water via centrifugation and filtration, dispersing in water finally. The content of dry matter was determined by drying a definite of GO or rGO dispersion at 70 °C.

Synthesis of MnO_2/Graphene Nanocomposite Electrode Materials. A series of MnO_2/graphene nanocomposites with different feeding ratios (mass ratio of SBP and GO or rGO of 1:10, 1:5, 1:1, 5:1, and 10:1) was synthesized by physically mixing SBP and GO or rGO. For instance, the preparation of the SBP/GO (1:10) nanocomposite was conducted as follows: 50 mL of GO dispersion (0.4 mg/mL) and 2 mg of SBP in 50 mL deionized water were ultrasonicated for 30 min, respectively, followed by the combination of the two components

DOI: 10.1021/acssuschemeng.5b00305
ACS Sustainable Chem. Eng. 2015, 3, 1330−1338

under sonication for another 30 min. Next, the mixture was stirred for 8 h. Finally, the nanocomposite was obtained by centrifugation and drying in a vacuum at 45 °C.

Characterization. The morphologies of the samples were characterized by a TEM (JEOL, Tokyo, Japan) operating at an accelerating voltage of 100 kV. The samples were dispersed in ethanol by ultrasonication and dropped onto the Cu grids covered with a polymer film for analysis. SEM was studied with an s-4800 scanning electron microscope (SEM, Hitachi, Japan). The sample used for SEM observation was performed by placing drops of the SBP/rGO (5:1) suspension onto a silicon wafer. Then, a small amount of Au was vaporized onto the surface of samples for a clear photograph after drying in a vacuum.

The X-ray diffraction (XRD) patterns were recorded in the 2θ range of 10°−80° by step scanning with a PANalytical X'Pert PRO X-ray diffractometer (PANalytical, Almelo, The Netherlands).

Fourier transform infrared (FT-IR) spectroscopy analysis was performed in the range of 400−4000 cm^{-1} with a resolution of 4 cm^{-1} using the KBr pellet technique on a Bruker IFS 66 v/s infrared spectrometer (Bruker, Karlsruhe, Germany).

Raman spectra measurements were carried out on a Horiba Jobin-Yvon LabRAM HR 800 UV apparatus using an excitation laser with a wavelength of 532 nm.

The electrochemical performance tests were carried out on a CHI660E electrochemical workstation (CHI, Shanghai) using a traditional three electrode system and 1 mol/L Na_2SO_4 as an electrolyte, including a working electrode (composites samples), a counter electrode (platinum plate), and a reference electrode (Hg/Hg_2Cl_2). The working electrodes were prepared via mixing the active materials, carbon black, and polyvinylidenefluoride (PVDF) with a mass ratio of 80:15:5 in N,N-dimethylformamide (DMF). Then, the slurry was uniformly painted on a stainless steel mesh (current collector) with an area of about 0.25 cm^2. The amount of the active materials on the electrode surface was determined from the weight difference before and after loading. Galvanostatic charge/discharge curves were measured at a constant current density of 1 A/g, and electrochemical impedance spectroscopy tests were carried out in the frequency range from 100 kHz to 0.01 Hz with an ac potential amplitude of 5 mV.

RESULTS AND DISCUSSION

MnO_2/Graphene Nanocomposites. The FT-IR spectrum shows the presence of the oxygen-containing groups at 3390, 1720, and 1230/1052 cm^{-1} for the GO, which are attributed to the −OH, C═O, and C−O in COH/COC (epoxy) functional groups, respectively (Figure 1a).[26] In the case of the rGO, the absorbance band of the carboxylic acid at 1720 cm^{-1} disappeared, and the C−O absorbance band (1230/1052 cm^{-1}) also decreased after processing a chemical reduction, which illustrated that the GO was successfully reduced to rGO. The peak at 572 cm^{-1} assigned to the Mn−O stretching vibration[13] can also be observed in the SBP/rGO(5:1), indicating the presence of MnO_2 nanoparticles.

The Raman spectra display two prominent peaks at 1350 cm^{-1} (D band corresponding to sp^3-hybridized carbon) and 1598 cm^{-1} (G band related to sp^2-hybridized carbon; Figure 1b).[27,28] What's more, the intensity ratio of the D to G bands (I_D/I_G) reflecting the graphitization degree of carbonaceous materials and the defect density decreased after processing a chemical reduction, suggesting the successful reduction of GO.[29]

The XRD patterns of the samples are shown in Figure 1c. For the rGO, a broad peak around 25° could be seen, suggesting most of the oxygen-containing groups have been removed via a chemical reduction,[14,30] as well as the peak at 2θ around 43° corresponding to the (100) crystal plane of graphene.[31] As for the rGO, the diffraction peak at a 2θ value of

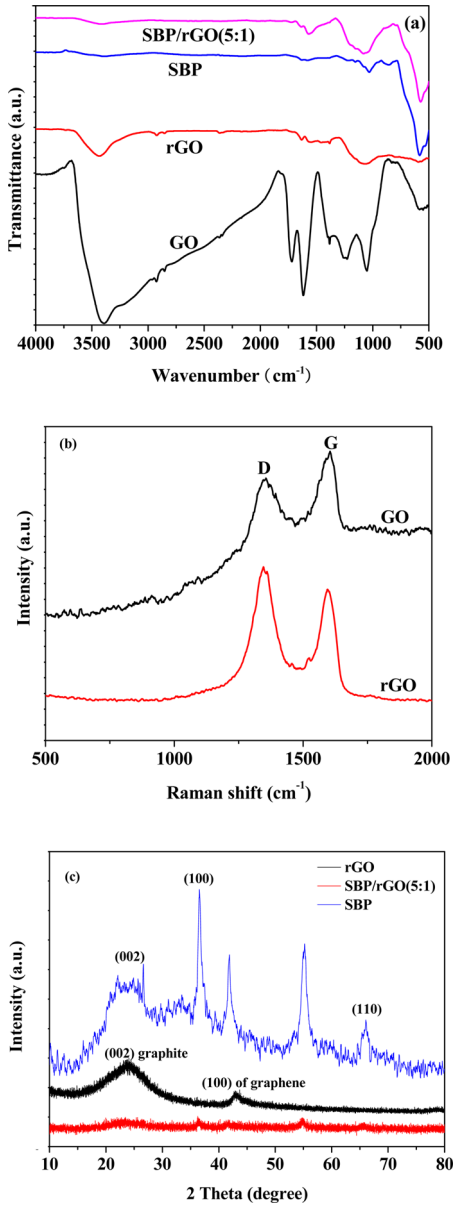

Figure 1. (a) FT-IR spectra of the SBP, GO, rGO, and SBP/rGO(5:1) with a feeding ratio of SBP and rGO of 5:1. (b) Raman spectra of the GO and rGO. (c) Typical XRD patterns of the SBP, rGO, and SBP/rGO(5:1) with a feeding ratio of SBP and rGO of 5:1.

25° can be ascribed to the (002) planes of graphite, which was also observed in rGO.[31] The significant patterns at 2θ = 24.5°, 36.6°, and 66° could be respectively well-assigned to the (002), (100), and (110) planes of birnessite-type MnO_2.[13,14] The wide peaks and the presence of other patterns indicated that the SBP did not consist of only birnessite-type MnO_2, and the crystallinity of the birnessite-type MnO_2 was also not perfect. In the case of the SBP/rGO(5:1) nanocomposites, the patterns at 25° and 36.6° demonstrated the coexistence of rGO and SBP in the composites. However, the peak at 43° cannot be observed, which might be a result of the low graphitization degree due to the deposition of MnO_2 onto the graphene.[13,14]

The morphology of the obtained SBP is shown in Figure 2g. It can be seen that the nanoparticles are about 20−100 nm in diameter. Additionally, some block or sheets can also be observed in the image, assigned to the graphite flake. The

DOI: 10.1021/acssuschemeng.5b00305
ACS Sustainable Chem. Eng. 2015, 3, 1330−1338

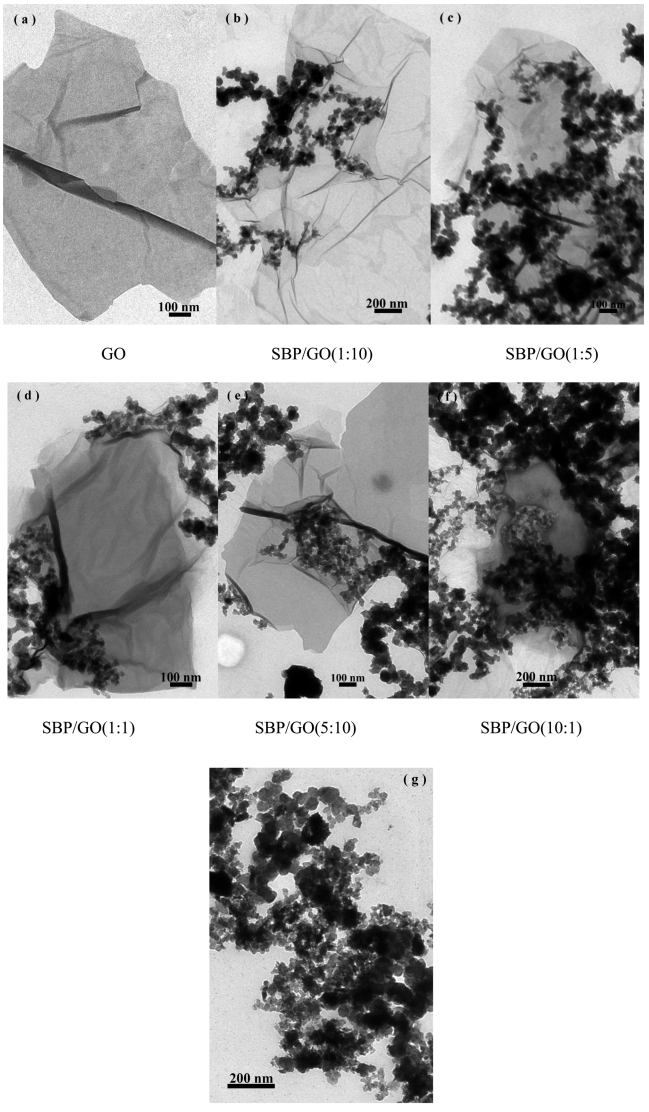

Figure 2. TEM images of SBP/GO nanocomposites with different mass ratios of SBP and GO (a–f) and SBP obtained from waste Zn-MnO_2 dry battery (g).

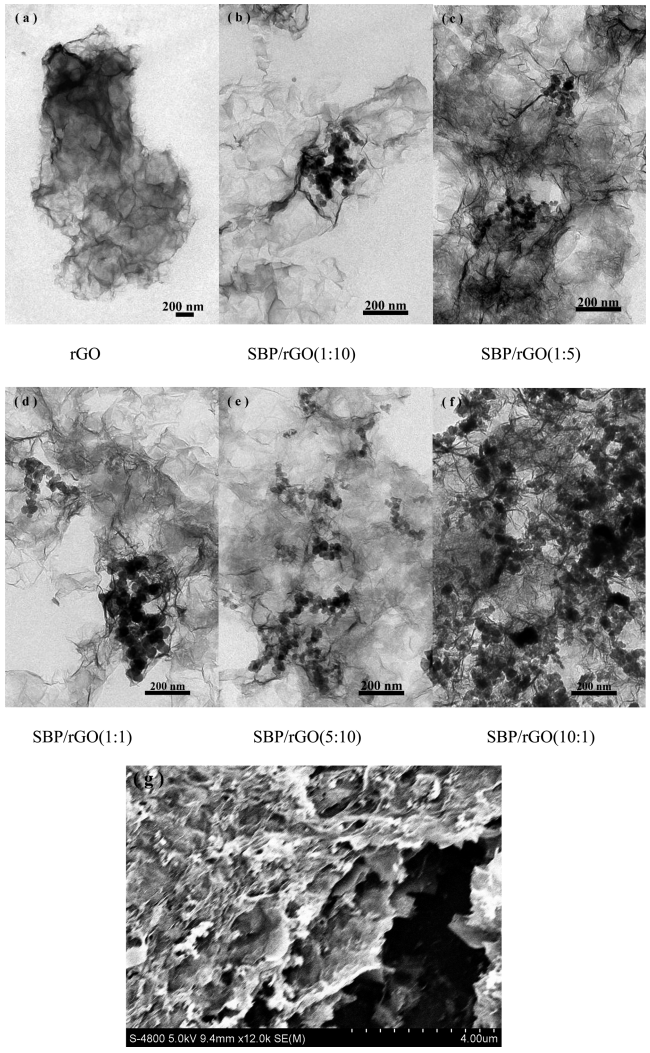

Figure 3. TEM images of the SBP/rGO nanocomposites with different mass ratios of SBP and rGO (a–f) and SEM image of the as-prepared SBP/rGO(5:1) nanocomposite prepared with a mass ratio of SBP to rGO of 5:1 (g).

microstructure of the pristine GO or rGO and the resulting nanocomposites are demonstrated in Figures 2 and 3. As seen from the image in Figure 2a, the GO was smooth and transparent as thin layers; however, the rGO sheets tended to be wrinkled and stacked together loosely as shown in Figure 3a,[13] which might be due to van der Waals interaction. At the same time, a higher specific area was achieved by the loosely stacked structure creating a number of voids and cavities (Figure 3a). All the micrographs showed that the spherical nanoparticles had been anchored on the GO or rGO sheets as shown in Scheme 1, and their number increased with the increase in the feeding ratio of the SBP. The nanoparticles tended to assemble at the edges and basal planes of the GO due to the oxygen functional groups in spite of some being located at the blank region.[11] In the case of the SBP/rGO(10:1) nanocomposite, however, the nanoparticles seemed to aggregate and be wrapped by the rGO sheets because of the high specific surface area and van der Waals interaction. The SEM image also showed that the rGO with high surface area might be a substrate for the SBP to form a 2D nanostructure (Figure 3g), acting as the support for the MnO_2 nanoparticles. As a result, the capacitance property was improved.

Electrochemical Properties. Figure 4 a and b show the galvanostatic charge/discharge (GCD) curves of the pristine GO, rGO, and SBP and the resulting nanocomposite electrodes in the potential range of −0.2 to 0.8 V. It can be seen that all curves showed a small IR drop revealing the internal resistance of materials was low. What is more, from the shape of these GCD curves, it showed mainly a double-layer capacitance behavior of the nanocomposites with a higher percentage of the GO or rGO. The specific capacitance of the original SBP is 66 F/g, which is largely lower than the theoretical specific capacitance value of MnO_2. The reason might be presumably ascribed to its imperfect crystal and the impurities presented in the powders and the loss of activity of MnO_2 compared to the new-made MnO_2 after the redox process. However, the capacitance performance was largely improved after mixing with the GO or rGO; for instance, the specific capacitances of the SBP/GO(5:1) (118 F/g) and SBP/rGO(5:1) (150 F/g) are 2 and 2.5 fold higher than that of the pristine SBP (66 F/g), as shown in Figure 4c.

DOI: 10.1021/acssuschemeng.5b00305
ACS Sustainable Chem. Eng. 2015, 3, 1330–1338

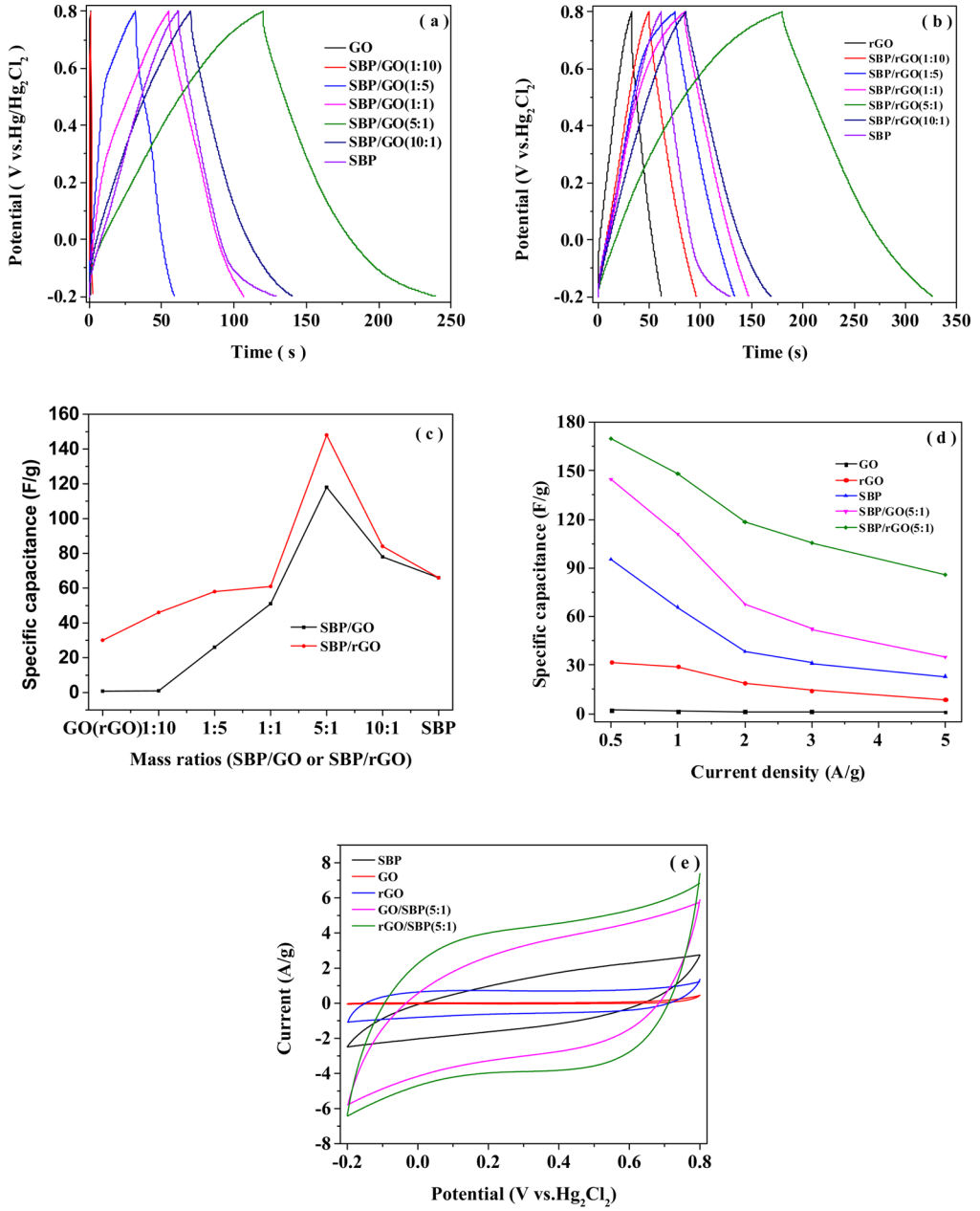

Figure 4. Galvanostatic charge/discharge curves of the SBP/GO (a) and SBP/rGO (b) nanocomposite electrodes at a current density of 1 A/g. Specific capacitances of samples as a function of composition (c) and different discharge current densities (d) at 0.5−5A/g in 1 mol/L Na_2SO_4 solution. (e) Cyclic voltammetry curves of the SBP, GO, and rGO and the nanocomposite electrodes at 100 mV/s in 1 mol/L Na_2SO_4 aqueous solution.

Figure 4c depicts the variation of specific capacitance with the mass ratio of the SBP and GO or rGO. It can be seem that the specific capacitance of the resultant nanocomposite electrodes can be only enhanced at a high mass ratio of the SBP and GO or rGO due to the poor capacitive performance of the GO or rGO. The specific capacitances of the GO and rGO are 1 F/g and 30 F/g at a discharge current of 1 A/g, respectively. Additionally, the capacitance improvement of the composites largely depends on the mass ratio of the SBP and GO or rGO; in other words, the distribution of the MnO_2 phase and the morphology of the nanocomposites affected the electrochemical performance of such nanocomposites.[18] The nanocomposites synthesized at a mass ratio of 5:1 exhibited a most excellent capacitive performance, with a specific capacitance of 118 F/g for the SBP/GO(5:1) nanocomposite electrode and 150 F/g for the SBP/rGO(5:1) nanocomposite electrode, which is about 2 times higher than that of the pristine SBP (66 F/g), as shown in Figure 4c.

The rate capacity of these composites was also characterized by GCD technique under different current densities (Figure 4d). The specific capacitance of the electrodes decreased with increasing the discharge current densities from 0.5 to 5 A/g. At a high current density, the hydrated ions are mainly adsorbed on the outer surface of the electrode, while they can approach deep pores of the supercapacitor electrodes leading to higher capacity at a low current density, which was mainly due to the limited ion migration into the internal structure of the electrode material as the current density increased.[32] Compared with the

DOI: 10.1021/acssuschemeng.5b00305
ACS Sustainable Chem. Eng. 2015, 3, 1330−1338

Table 1. Summary of the Supercapacitors Based on the MnO_2-Graphitic Electrode Materials Reported in the Contemporary Literature

electrode materials	preparation method	capacatance (F/g)	cycle stability	energy/power density (Wh/kg, kW/kg)	ref
MnO_2/graphene[a]	hydrothermal method, 140 °C for 2 h	197.3 F/g at 100 mV/s	8.9% loss after 1000 cycles		36
MnO_2 nanowire−rGO[a]	hydrothermal method, 83 °C for 30 min in isopropyl alcohol/H_2O	111.1 F/g at 1 A/g	15.9% loss after 1000 cycles		11
graphene//MnO_2 nanowire-graphene asymmetric EC[b]	solution phase assembly of graphene sheets and MnO_2-nanowires at 70 °C for 6 h	31 F/g at 0.5 A/g	21% loss after 1000 cycles	30.4/5	12
graphene-wrapped MnO_2 Nanospheres[b]	electrostatic coassembly between positively charged MnO_2 nanospheres and negatively charged graphene	210 F/g at 0.5 A/g	17.6% loss after 1000 cycles		13
MnO_2/graphitic petals/ buckypaper[c]	chemical redox deposition at 80 °C for 40 min and 200 °C for 2 h	580 F/g at 2 mV/s	10% loss after 1000 cycles	28/25 at 50 A/g	39
manganese oxide-graphite[c]	chemical redox deposition, graphite foil was immersed in the solution of $KMnO_4$	556 mF/cm^2 at 10 mV/s	10% loss after 300 cycles		37
MnO_2−rGO/flexible carbon fiber paper[d]	physical mixing of rGO nanosheets and MnO_2 nanoparticles	393 F/g at 0.1 A/g	1.5% loss after 2000 cycles		17
SBP/rGO(5:1)[d]	physical mixing of rGO nanosheets and spent battery powders (SBP) at room temperature	150 F/g at 1A/g	6.3% loss after 1000 cycles		present work

[a]The adsorption or anchoring of Mn^{2+} on the GO acting as nucleation centers first by the oxygenated functional groups of GO; subsequently the MnO_2 was formed in situ by hydrothermal oxidation reaction. (Reaction equation: $2MnO_4^- + 3Mn^{2+} + 2H_2O = 5MnO_2 + 4H^+$.) [b]The manganese oxide was fabricated in advance and then subjected to modification to enhance the interactions between the graphene sheets and metal oxide. [c]MnO_2 was deposited onto the surface of graphene by a redox reaction, in which $KMnO_4$ was reduced to MnO_2 by the sacrifice of graphene carbon. (Reaction equation: $4MnO_4^- + 3C + H_2O = 4MnO_2 + CO_3^{2-} + 2HCO_3^-$.) [d]Physical mixing of colloidal MnO_2 nanoparticles and rGO to prepare MnO_2-rGO nanocomposites.

other samples, the SBP/rGO nanocomposite electrodes showed the highest specific capacitance under all the current densities indicating good rate capacity, which might be a result from the synergistic effect of the rGO (high specific surface and conductivity) and battery powder (pseudocapacitor). Moreover, the specific capacitances of the SBP/rGO nanocomposite electrodes were higher than those of the SBP/GO nanocomposite electrodes under all the measured current densities because the SBP also can be decorated on the reduced graphene due to the remaining oxygen-containing groups after reduction.[33] Most importantly, the rGO has higher electrical conductivity, which is favorable for the transport of the hydrated ions.[17,34]

Figure 4e displays the CV curves of the SBP, GO, and rGO and the nanocomposite electrodes at a scan rate of 100 mV/s. It is clear that the specific capacitance is proportional to the areas of a CV curve, revealing that the SBP/rGO(5:1) nanocomposite electrode has the highest specific capacitance, which can be attributed to the synergistic effect of the rGO and MnO_2, where rGO can improve the electrical conductivity of MnO_2 and the MnO_2 contributes high capacitance through a redox reaction process. The CV and GCD curves showed that the capacitance of the neat GO or rGO electrode was poor, so the GO or rGO might not contribute prominently to the total capacitance of the electrode materials. Nevertheless, their presence helped the MnO_2 nanoparticles to disperse over a large area resulting in the increase of electrochemically active sites for effective redox reactions of MnO_2 and then improving the utilization ratio of MnO_2.[35,18] Therefore, the carbon materials might act as a supports mainly for the SBP to form a 2D nanostructure, leading to an improvement of specific capacitance.

A summary of the preparation method of the MnO_2-graphitic electrode materials and the corresponding electrochemical data is shown in Table 1. Although it is difficult to obtain a precise comparison of electrochemical performance of an electrode material, the data were recorded with different parameters (eg., testing systems and method, electrolyte, and the fabrication of electrode). The SBP/rGO(5:1) nanocomposite electrode in the present work tended to a better chemical performance compared to the others because of just losing 6.3% of its initial capacitance after 1000 cycles and a moderate capacitance which was obtained at a higher discharge current densities (1 A/g). Most importantly, the preparation method in the present work is very simple, in which the spent battery powder (SBP) was recycled as the main raw material.

Figure 5 presents the CV and galvanostatic charge/discharge curves of the SBP/rGO(5:1) nanocomposite electrode at different scan rates or current densities. The CV curves showed a nearly rectangular and symmetric shape, indicating the ideal capacitive behavior,[36] and the CV curves were distorted with increasing scan rates due to the contributions of the combined double-layer and pseudocapacitive capacitances.[38] The symmetrical GCD curves demonstrated that the electrochemical process of charge/discharge was reversible superiorly at different current densities. What is more, the potential drop was small in all the curves.[31]

Figure 6a displays the electrochemical impedance spectra of the GO, rGO, SBP/GO(5:1), and SBP/rGO(5:1) nanocomposite electrodes. The impedance curves showed an inclined line in the low-frequency region and a compressed semicircle in the medium-frequency region.[40] It can be found that the resistance of the SBP was the lowest among the other electrodes, about 18 Ω, which might be a result of the fine structure and the improved electrical electricity by graphite powders presented in the battery powder, while the GO and rGO displayed a higher impedance. In the case of the nanocomposites, the impedance decreased after the incorporation of carbon substrate and spent battery powder, indicating the enhancement of conductivity. Therefore, in consideration of the overall performance, the SBP played an important role in the enhancement of electrochemical performance of the nanocomposite electrodes because the pristine SBP has the lowest resistance and the best cyclic stability, so the GO or rGO

DOI: 10.1021/acssuschemeng.5b00305
ACS Sustainable Chem. Eng. 2015, 3, 1330−1338

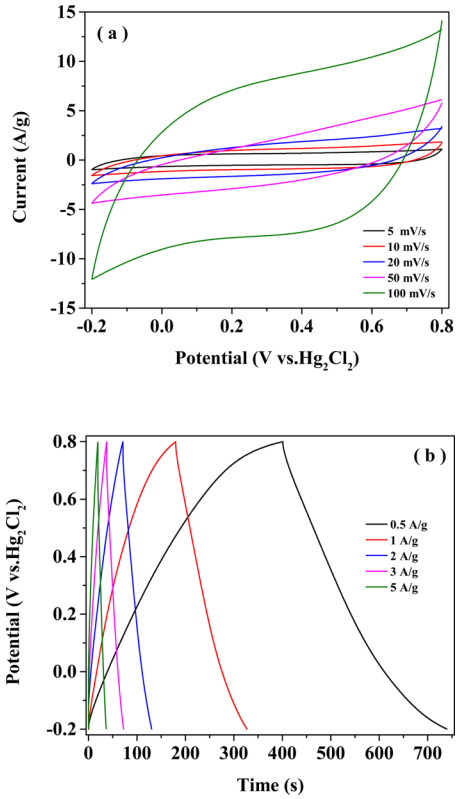

Figure 5. (a) Cyclic voltammetry and (b) charge/discharge curves of the SBP/rGO(5:1) nanocomposite electrode at different scan rates or current densities in 1 mol/L Na_2SO_4 aqueous electrolyte.

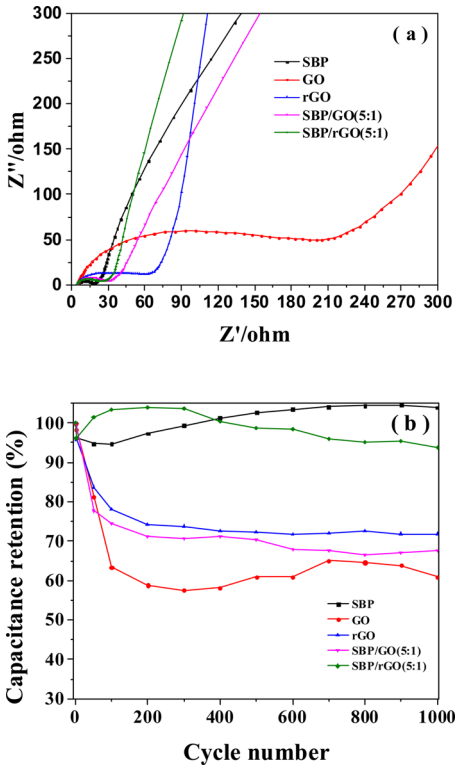

Figure 6. (a) EIS curves of samples in the frequency range of 100 kHz to 0.01 Hz. (b) Cycle life of the samples upon CVs measured at a scan rate of 100 mV/s in 1 mol/L Na_2SO_4 aqueous solution.

might only act as a a substrate for the SBP to form a 2D nanostructure, leading to an improvement of specific capacitance.

The long-term cycle stabilities of these electrodes were investigated by cyclic voltammogram (CV) tests for 1000 cycles in 1 mol/L Na_2SO_4 aqueous solution, as shown in Figure 6 b. After 1000 CV cycles, the specific capacitance retention of the SBP electrode retained over 100%, exhibiting excellent cyclic stability due to the fine nanostructure of graphite and MnO_2 nanoparticles relaxing the mechanical stress generated during intercalation/deintercalation of the electrolyte ions.[41,42] Nevertheless, the specific capacitance of the GO or rGO was only kept about 70% of the original capacitance. In the case of the nanocomposites, the cycling stability of the SBP/GO(5:1) had been improved slightly, while the SBP/rGO(5:1) had been largely enhanced to be more than 90%, compared to the pure GO and rGO, respectively.

CONCLUSIONS

In summary, spent battery powder (SBP) containing graphite and MnO_2 nanoparticles, obtained via a simple process from the waste acidic dry batteries, was recycled for the MnO_2/graphene nanocomposites just through a facile physical mixing method. The electrochemical tests showed that the SBP exhibited excellent cyclic stability, keeping 100% of its original capacitance after 1000 cycles and low impedance compared to the graphene oxide (GO) or reduced graphene oxide (rGO). In the case of the resultant nanocomposite electrodes, the specific capacitance depended on the mass ratio of SBP and GO or rGO, and the highest specific capacitance was achieved when the mass ratio of SBP and GO or rGO was 5:1. The highest specific capacitance, 118 F/g for the SBP/GO (5:1) nanocomposite electrode and 150 F/g for the SBP/rGO (5:1) nanocomposite electrode, is about 2 times higher than that of the pristine SBP electrode (66 F/g). What is more, the specific capacitances of the SBP/rGO nanocomposite electrodes were higher than those of the SBP/GO nanocomposite electrodes at the same mass ratios. In consideration of the structure and composition of the SBP, the capacitance can be improved furthermore if the MnO_2 in the SBP was treated to improve its purity and/or crystalline, so it is reasonable to design a structure and composition like this to achieve a promising electrochemical performance. Therefore, this present investigation would bring the waste batteries a new life for energy storage and transformation.

AUTHOR INFORMATION

Corresponding Author

*Tel./Fax: 86 0931 8912582. E-mail: pliu@lzu.edu.cn.

Notes

The authors declare no competing financial interest.

ACKNOWLEDGMENTS

This work was supported by the Open Project of the Joint Research Center of Urban Resource Recycling Technology of Graduate School at Shenzhen, Tsinghua University and Shenzhen Green Eco-Manufacturer High-Tech (No. URRT2014001).

REFERENCES

(1) Simon, P.; Gogotsi, Y. Materials for electrochemical capacitors. *Nat. Mater.* **2008**, 7 (11), 845−854.

DOI: 10.1021/acssuschemeng.5b00305
ACS Sustainable Chem. Eng. 2015, 3, 1330−1338

(2) Miller, J. R.; Simon, P. Electrochemical capacitors for energy management. *Science* **2008**, *321* (5889), 651−652.
(3) Kotz, R.; Carlen, M. Principles and applications of electrochemical capacitors. *Electrochim. Acta* **2000**, *45* (15/16), 2483−2498.
(4) Hall, P. J.; Mirzaeian, M.; Fletcher, S. I.; Sillars, F. B.; Wilson, G.; Cruden, A.; Carter, R. Energy storage in electrochemical capacitors: designing functional materials to improve performance. *Energy Environ. Sci.* **2010**, *3* (9), 1238−1251.
(5) Stoller, M. D.; Park, S.; Zhu, Y.; An, J.; Ruoff, R. S. Graphene-based ultracapacitors. *Nano Lett.* **2008**, *8* (10), 3498−3502.
(6) Chen, J.; Li, C.; Shi, G. Q. Graphene materials for electrochemical capacitors. *J. Phys. Chem. Lett.* **2013**, *4* (8), 1244−12535.
(7) Xu, M.; Kong, L.; Zhou, W.; Li, H. Hydrothermal synthesis and pseudocapacitance properties of α-MnO_2 hollow spheres and hollow urchins. *J. Phys. Chem. C* **2007**, *111* (51), 19141−19147.
(8) Fischer, A. E.; Pettigrew, K. A.; Rolison, D. R.; Stroud, R. M.; Long, J. W. Incorporation of homogeneous, nanoscale MnO_2 within ultraporous carbon structures via self-limiting electroless deposition: implications for electrochemical capacitors. *Nano Lett.* **2007**, *7* (2), 281−286.
(9) Chen, Y. L.; Hu, Z. A.; Chang, Y. Q.; Wang, H. W.; Zhang, Z. Y.; Yang, Y. Y.; Wu, H. Y. Zinc oxide/reduced graphene oxide composites and electrochemical capacitance enhanced by homogeneous incorporation of reduced graphene oxide sheets in zinc oxide matrix. *J. Phys. Chem. C* **2011**, *115* (5), 2563−2571.
(10) Gund, G. S.; Dubal, D. P.; Patil, B. H.; Shinde, S. S.; Lokhande, C. D. Enhanced activity of chemically synthesized hybrid graphene oxide/Mn_3O_4 composite for high performance supercapacitors. *Electrochim. Acta* **2013**, *92*, 205−215.
(11) Chen, S.; Zhu, J.; Wu, X.; Han, Q. F.; Wang, X. Graphene oxide-MnO_2 nanocomposites for supercapacitors. *ACS Nano* **2010**, *4* (5), 2822−2830.
(12) Wu, Z. S.; Ren, W.; Wang, D. W.; Li, F.; Liu, B.; Cheng, H. M. High-energy MnO_2 nanowire/graphene and graphene asymmetric electrochemical capacitors. *ACS Nano* **2010**, *4* (10), 5835−5842.
(13) Zhu, J.; He, J. Facile synthesis of graphene-wrapped honeycomb MnO_2 nanospheres and their application in supercapacitors. *ACS Appl. Mater. Interfaces* **2012**, *4* (3), 1770−1776.
(14) Yan, J.; Fan, Z.; Wei, T.; Qian, W. Z.; Zhang, M. L.; Wei, F. Fast and reversible surface redox reaction of graphene−MnO_2 composites as supercapacitor electrodes. *Carbon* **2010**, *48* (13), 3825−3833.
(15) Lee, J. W.; Hall, A. S.; Kim, J. D.; Mallouk, T. E. A facile and template-free hydrothermal synthesis of Mn_3O_4 nanorods on graphene sheets for supercapacitor electrodes with long cycle stability. *Chem. Mater.* **2012**, *24* (6), 1158−1164.
(16) Li, S. M.; Wang, Y. S.; Yang, S. Y.; Liu, C. H.; Chang, K. H.; Hu, C. C. Electrochemical deposition of nanostructured manganese oxide on hierarchically porous graphene-carbon nanotube structure for ultrahigh-performance electrochemical capacitors. *J. Power Source* **2013**, *225*, 347−355.
(17) Sawangphruk, M.; Srimuk, P.; Chiochan, P.; Krittayavathananon, A.; Luanwuthi, S.; Limtrakul, J. High-performance supercapacitor of manganese oxide/reduced graphene oxide nanocomposite coated on flexible carbon fiber paper. *Carbon* **2013**, *60*, 109−116.
(18) Hsieh, C. T.; Lee, W. Y.; Lee, C. E.; Teng, H. Electrochemical capacitors fabricated with tin oxide/graphene oxide nanocomposites. *J. Phys. Chem. C* **2014**, *118* (28), 15146−15153.
(19) McMichael, F. C.; Henderson, C. Recycling batteries. *IEEE Spectrum* **1998**, *35* (2), 35−42.
(20) Qu, J.; Feng, Y.; Zhang, Q.; Cong, Q.; Luo, C. Q.; Yuan, X. A new insight of recycling of spent Zn-Mn alkaline batteries: Synthesis of $Zn_xMn_{1-x}O$ nanoparticles and solar light driven photocatalytic degradation of bisphenol A using them. *J. Alloys Compd.* **2015**, *622*, 703−707.
(21) Brito, P. S. D.; Patrício, S.; Rodrigues, L. F.; Sequeira, C. A. C. Electrodeposition of Zn−Mn alloys from recycling Zn−MnO_2 batteries solutions. *Surf. Coat. Technol.* **2012**, *206* (13), 3036−3047.
(22) Sayilgan, E.; Kukrer, T.; Civelekoglu, G.; Ferella, F.; Akcil, A.; Veglio, F.; Kitis, M. A review of technologies for the recovery of metals from spent alkaline and Zinc-carbon batteries. *Hydrometallurgy* **2009**, *97* (3−4), 158−166.
(23) Hummers, W. S.; Offeman, R. E. Preparation of graphitic oxide. *J. Am. Chem. Soc.* **1958**, *80* (6), 1339.
(24) Sun, X. M.; Liu, Z.; Welsher, K.; Robinson, J. T.; Goodwin, A.; Zaric, S.; Dai, H. J. Nano-graphene oxide for cellular imaging and drug delivery. *Nano Res.* **2008**, *1* (3), 203−212.
(25) Li, D.; Müller, M. B.; Gilje, S.; Kaner, R. B.; Wallace, G. G. Processable aqueous dispersions of graphene nanosheets. *Nat. Nanotechnol.* **2008**, *3* (2), 101−105.
(26) Titelman, G. I.; Gelman, V.; Bron, S.; Khalfin, R. L.; Cohen, Y.; Peled, H. B. Characteristics and microstructure of aqueous colloidal dispersions of graphite oxide. *Carbon* **2005**, *43* (3), 641−649.
(27) Wang, H. L.; Robinson, J. T.; Li, X. L.; Dai, H. J. Solvothermal reduction of chemically exfoliated graphene sheets. *J. Am. Chem. Soc.* **2009**, *131* (29), 9910−9911.
(28) Kudin, K. N.; Ozbas, B.; Schniepp, H. C.; Prud'homme, R. K.; Aksay, I. A.; Car, R. Raman spectra of graphite oxide and functionalized graphene sheets. *Nano Lett.* **2008**, *8* (1), 36−41.
(29) Zhao, W. F.; Fang, M.; Wu, F. L.; Wu, H.; Wang, L. W.; Chen, G. H. Preparation of graphene by exfoliation of graphite using wet ball milling. *J. Mater. Chem.* **2010**, *20* (28), 5817−5819.
(30) Zhang, J. T.; Jiang, J. W.; Zhao, X. S. Synthesis and capacitive properties of manganese oxide nanosheets dispersed on functionalized graphene sheets. *J. Phys. Chem. C* **2011**, *115* (14), 6448−6454.
(31) Yang, S. H.; Song, X. F.; Zhang, P.; Gao, L. Facile synthesis of nitrogen-doped graphene-ultrathin MnO_2 sheet composites and their electrochemical performances. *ACS Appl. Mater. Interfaces* **2013**, *5* (8), 3317−3322.
(32) Yang, L.; Cheng, S.; Ding, Y.; Zhu, X. B.; Wang, Z. L.; Liu, M. L. Hierarchical network architectures of carbon fiber paper supported cobalt oxide nanonet for high-capacity pseudocapacitors. *Nano Lett.* **2012**, *12* (1), 321−325.
(33) Li, Y.; Zhao, N. Q.; Shi, C. S.; Liu, N.; He, C. Improve the supercapacity performane of MnO_2-decorated graphene by controlling the oxidization extent of graphene. *J. Phys. Chem. C* **2012**, *116* (48), 25226−25232.
(34) Peng, L.; Peng, X.; Liu, B.; Wu, C. Z.; Xie, Y.; Yu, G. H. Ultrathin two-dimensional MnO_2/graphene hybrid nanostructures for high-performance, flexible planar supercapacitors. *Nano Lett.* **2013**, *13* (5), 2151−2157.
(35) Sharma, R. K.; Oh, H. S.; Shul, Y. G.; Kim, H. Carbon-supported, nano-structured, manganese oxide composite electrode for electrochemical supercapacitor. *J. Power Source* **2007**, *173* (2), 1024−1028.
(36) Feng, X. M.; Yan, Z. Z.; Chen, N. N.; Zhang, Y.; Ma, Y. W.; Liu, X. F.; Fan, Q. L.; Wang, L. H.; Huang, W. The synthesis of shape-controlled MnO_2/graphene composites via a facile one-step hydrothermal method and their application in supercapacitors. *J. Mater. Chem. A* **2013**, *1* (41), 12818−12825.
(37) Xiong, G. P.; Hembram, K.; Reifenberger, R. G.; Fisher, T. S. MnO_2-coated graphitic petals for supercapacitor electrodes. *J. Power Source* **2013**, *227*, 254−259.
(38) Lin, C. C.; Chen, H. W. Coating manganese oxide onto graphite electrodes by immersion for electrochemical capacitors. *Electrochim. Acta* **2009**, *54* (11), 3073−3077.
(39) Chen, H.; Zhou, S. X.; Chen, M.; Wu, L. M. Reduced graphene oxide−MnO_2 hollow sphere hybrid nanostructures as high-performance electrochemical capacitors. *J. Mater. Chem.* **2012**, *22* (48), 25207−25216.
(40) Cui, L. F.; Shen, J.; Cheng, F. Y.; Tao, Z. L.; Chen, J. SnO_2 nanoparticles@polypyrrole nanowires composite as anode materials for rechargeable lithium-ion batteries. *J. Power Source* **2011**, *196* (4), 2195−2201.
(41) Kravchyk, K.; Protesescu, L.; Bodnarchuk, M. I.; Krumeich, F.; Yarema, M.; Walter, M.; Guntlin, C.; Kovalenko, M. V. Monodisperse and inorganically capped Sn and Sn/SnO_2 nanocrystals for high-

DOI: 10.1021/acssuschemeng.5b00305
ACS Sustainable Chem. Eng. 2015, 3, 1330−1338

performance Li-ion battery anodes. *J. Am. Chem. Soc.* **2013**, *135* (11), 4199−4202.
(42) Zhang, K.; Wang, L. J.; Hu, Z.; Cheng, F. Y.; Chen, J. Ultrasmall Li_2S nanoparticles anchored in graphene nanosheets for high-energy lithium-ion batteries. *Sci. Rep.* **2014**, *4* (9), 6467−6473.

NOTE ADDED AFTER ASAP PUBLICATION

This article was published ASAP on June 2, 2015, without all of the corrections. The corrected article was published ASAP on June 8, 2015.

DOI: 10.1021/acssuschemeng.5b00305
ACS Sustainable Chem. Eng. 2015, 3, 1330−1338